https://doi.org/10.5194/amt-2021-333
Preprint. Discussion started: 20 October 2021

Atmospheric Measurement Techniques Discussions

Identification of Smoke and Sulfuric Acid Aerosol in SAGE III/ISS Extinction Spectra Following the 2019 Raikoke Eruption

Travis N. Knepp[1], Larry Thomason[1], Mahesh Kovilakam[2,1], Jason Tackett[1], Jayanta Kar[2,1], Robert Damadeo[1], and David Flittner[1]

[1]NASA Langley Research Center, Hampton, Virginia 23681, USA
[2]Science Systems and Applications, Inc. Hampton, Virginia 23666, USA

Correspondence: Travis N. Knepp (travis.n.knepp@nasa.gov)

Abstract. The 2019 eruption of Raikoke was the largest volcanic eruption since 2011 and it was coincident with 2 major wildfires in the northern hemisphere. The impact of these events was manifest in the SAGE III/ISS extinction coefficient measurements. As the volcanic aerosol layers moved southward, a secondary peak emerged at an altitude higher than that which is expected for sulfuric acid aerosol. It was hypothesized that this secondary plume may contain a non-negligible amount of smoke contribution. We developed a technique to classify the composition of enhanced aerosol layers as either smoke or sulfuric acid aerosol. This method takes advantage of the different spectral properties of smoke and sulfuric acid aerosol, which is manifest in distinctly different spectral slopes in the SAGE III/ISS data. Herein we demonstrate the utility of this method using 4 case-study events (2018 Ambae eruption, 2019 Ulawun eruption, 2017 Canadian pyroCb, and 2020 Australian pyroCb) and provide corroborative data from the CALIOP instrument before applying it to the Raikoke plumes. We determined that, in the time period following the Raikoke eruption, smoke and sulfuric acid aerosol were present throughout the atmosphere and the 2 aerosol types were preferentially partitioned to higher (smoke) and lower (sulfuric acid) altitudes. Herein, we present an evaluation of the performance of this classification scheme within the context of the aforementioned case-study events followed by a brief discussion of this method's applicability to other events as well as its limitations.

1 Introduction

Located on the Kuril archipelago, Raikoke (48.3°N, 153.3°E) is a volcanic island that has a history of moderately-sized eruptions that have been recorded over the last 200 years (Tanakadate, 1925; Newhall and Self, 1982; Rashidov et al., 2019). The 22-June, 2019 eruption was the largest volcanic eruption since 2011 (Puyehue-Cordón Caulle) and injected ≈1.5 Tg of sulfur dioxide (SO_2) into the lower stratosphere (Muser et al., 2020; de Leeuw et al., 2021). While the Raikoke eruption is interesting by itself, the time period surrounding the eruption is of particular interest because of coincident large wildfires in Russia and Canada (Kloss et al., 2021; Vaughan et al., 2021), resulting in the presence of smoke and volcanically derived material being present in the northern hemisphere's (NH) lower stratosphere at the same time. To better appreciate the recondite

https://doi.org/10.5194/amt-2021-333
Preprint. Discussion started: 20 October 2021


Atmospheric Measurement Techniques Discussions

synergistic significance of these events we have constructed this introduction in such a way as to inform the novice without distracting the cognoscenti. To this end, we will first put the magnitude of the Raikoke eruption into context with other eruptions followed by a brief discussion of the atmospheric impact of large wildfires. Finally, we will discuss the scientific interest of these coincident events for the current study and our motivation in conducting this study.

Stratospheric aerosol consists of submicron particles (Chagnon and Junge, 1961) that are composed primarily of sulfuric acid and water (Murphy et al., 1998) and play a crucial role in atmospheric chemistry and radiation transfer (Pitts and Thomason, 1993; Kremser et al., 2016; Wilka et al., 2018). Background stratospheric sulfuric acid is supplied by chronic, natural, emission of OCS (carbonyl sulfide), CS_2 (carbon disulfide), DMS (dimethyl sulfide), and SO_2 (sulfur dioxide), from both land and ocean sources (Kremser et al., 2016). The total amount of sulfur in the stratosphere is strongly modulated by volcanic activity. In the past few decades, this has most notably been the result of a few events like Pinatubo and El Chichón (McCormick et al., 1995). However, even relatively small events have been shown to impact stratospheric aerosol radiative forcing (Vernier et al., 2011), thus affecting climate and chemistry.

Volcanic eruptions have the potential to significantly change the atmosphere in several ways including changes in chemical composition, atmospheric dynamics, synoptic weather patterns, and radiation transfer. To facilitate comparison of volcanic events from a geological perspective, the Volcanic Explosivity Index (VEI) was developed by Newhall and Self (1982) and was later refined by Pyle (1995). While the VEI scale provides meaningful information for geologists (i.e., mass and volume of ejecta as well as rate of ejection), it retains little value for atmospheric scientists who are interested in what was ejected (e.g., SO_2, which is converted to sulfuric acid aerosol, as opposed to lava, rocks, and ash) and where the ejected material went (i.e., troposphere vs. stratosphere). However, the VEI scale remains in use by these scientists until a more meaningful scale is developed, ideally one that takes into consideration the climactic impact of these eruptions.

The VEI scale is based primarily on the volume of ejected tephra (solid material, not including gases) as described by Eq. 1 where V is the ejecta volume in cubic meters.

$$\text{VEI} = \log_{10}(V) - 4 \tag{1}$$

Therefore, for every integer step on the VEI scale the amount of ejecta increases by a factor of ten, making the largest eruptions (VEI >= 5) truly massive with ejecta volume on the order of cubic kilometers. To better appreciate the magnitude of the largest events the reader is encouraged to consider a few points: 1. the frequency of eruptions decreases approximately logarithmically as a function of VEI (VEI-7–8 occurring every 1000–2000 years), 2. on average, eruptions of a given VEI eject ≈40% more ejecta than an eruption on the next smaller VEI, 3. on average, eruptions with VEI-7 or VEI-8 are responsible for ≈50% of the total ejecta mass, ejecta volume, and thermal energy flux over the last 1000 years (Pyle, 1995).

The largest eruption within the last 500 years was the Mount Tambora eruption of 1815 (VEI-7), which released enough sulfur dioxide (SO_2), which was quickly converted to sulfuric acid aerosol in the stratosphere, to cool the northern hemisphere by up to 2 K. This resulted in the 1816 “year without summer” (Stothers, 1984; Schurer et al., 2019). Probably the best known eruption in recent history is the 1991 eruption of Mount Pinatubo (VEI-6), which resulted in a global temperature change of -1 K and changed the stratospheric aerosol levels for 7–9 years (Deshler et al., 2003; Santer et al., 2014). Therefore, despite being

https://doi.org/10.5194/amt-2021-333
Preprint. Discussion started: 20 October 2021


Atmospheric Measurement Techniques Discussions

relatively rare, large eruptions have a significant impact on short-term atmospheric chemistry and physics. However, it is not *just* large eruptions that influence atmospheric chemistry and radiative transfer. On the contrary, it has has been demonstrated that chronic eruptions of small volcanoes (VEI-3–4) play a measurable role as noted by Vernier et al. (2011), making them relevant to atmospheric chemistry and climate studies. While these eruptions lack the volume of their larger siblings, they make up for the difference in eruption frequency with VEI-3 eruptions taking place 4–5 times per year and VEI-4 eruptions occurring every 1-2 years. This results in a continual injection of SO_2, and sometimes ash, into the lower stratosphere and free troposphere, sometimes with devastating consequences. Possibly the most damaging eruption in this class was the Laki eruptions of 1783 (VEI-4) that consisted of both violent eruption events that resulted in plume heights of 15 km, and less-violent ejection of lava and gases that resulted in a volcanic fog (commonly referred to as vog). Continuing for 8 months, the Laki eruptions released a total of ≈120 Tg of SO_2, most of which remained within the troposphere (Thordarson and Self, 2003). To put this release of SO_2 in perspective, consider that the 1991 Pinatubo eruption (VEI-6) released only 20–30 Tg of SO_2 (Bluth et al., 1992; McCormick et al., 1995) and the 1815 eruption of Tambora (VEI-7) released ≈100 Tg of SO_2 (Pinto et al., 1989). Given the magnitude of SO_2 released, it is not surprising that the Laki eruption was responsible for the Icelandic "haze famine" wherein 20–25% of the Icelandic population died of starvation along with ≈60% of the grazing livestock (Thordarson and Self (1993, 2003) and references therein). This vog was also observed over England and Europe, possibly contributing to up to 20,000 additional deaths in England (Witham and Oppenheimer, 2004). While the loss of life has been attributed mainly to direct exposure to volcanic gases, it has been suggested that the stratospheric injections had significant climatological impact resulting in an unusually-cold winter throughout the entire northern hemisphere (Thordarson and Self, 2003). Though the extent of the climatological impacts have been called into question (D'Arrigo et al., 2011), the Laki eruptions serve as a prime example of how smaller eruptions can have significant impact on both life and climate.

Another source of stratospheric aerosol that has become significant over the past decade is large-scale, intense-burning, wildfire events that generate pyrocumulonimbus clouds (pyroCbs, also referred to as cumulonimbus flammagenitus), which were originally hypothesized to only exist as a product of nuclear explosions (Turco et al., 1983). These fires burn with sufficient intensity to form a cumulonimbus cloud and inject smoke and volatile organic compounds directly into the stratosphere (Fromm et al., 2006, 2010) on a scale comparable to a volcanic eruption of VEI-3–4 (Peterson et al., 2018). The largest pyroCbs on record are the 2017 Canadian and 2020 Australian wildfires, both of which injected between 0.1 and 0.9 Tg of aerosol into the lower stratosphere (Peterson et al., 2018; Yu et al., 2019; Kablick III et al., 2020).

These biomass burning events release black and brown carbon aerosol, which is carried into the stratosphere. Unlike sulfuric acid aerosol, black and brown carbon absorbs solar radiation causing it to heat throughout the day. Due to this diabatic heating, the density of the air mass immediately around the particles decreases, thereby lofting the smoke plume to higher altitudes, well past the initial injection height and independent of the general atmospheric circulation (Yu et al., 2019). This lofting effectively transports the chemical environment present in the lower atmosphere to higher altitudes, which can act as a tracer for pyroCb injections, as was demonstrated for the 2019/2020 Australian wildfires (Kablick III et al., 2020). Further, displacing the background stratospheric air with air that differs chemically and radiatively can also alter synoptic meteorology (Kablick III

https://doi.org/10.5194/amt-2021-333
Preprint. Discussion started: 20 October 2021


Atmospheric Measurement Techniques Discussions

et al., 2020). Therefore, while pyroCbs lack the eruptive power of volcanic events, they have the potential to play a substantive role in short-term ground-level air quality (Johnston et al., 2020) as well as stratospheric chemistry and dynamics.

Given the broad impact of these two event types, and the fact that they influence the atmosphere in distinctly different ways, it is necessary to be able to distinguish between the two.

A unique combination of volcanic and pyroCb events occurred in 2019 when the eruption of Raikoke was preceded by pyroCB events in Canada and Russia. This coincidence presented both a scientific opportunity as well as measurement challenges. Raikoke injected SO_2 and ash to a peak altitude of ≈15 km (Thomason et al., 2021), resulting in an SO_2 column density in excess of 900 Dobson units (Hedelt et al., 2019) and an overall mass load of ≈1.5 Tg (Muser et al., 2020; de Leeuw et al., 2021). This plume was transported to the northeast then down the western seaboard of North America before circling the globe (Hedelt et al., 2019; Chouza et al., 2020; Kloss et al., 2021; Vaughan et al., 2021). Herein we will show that part of the plume broke off from the main plume and continued to rise as it migrated equatorward, contrary to what has been previously observed for sulfuric acid aerosol, but is more typically associated with smoke. The working hypothesis is that this secondary plume consisted of wildfire smoke. The question we sought to answer is whether a positive identification of smoke in the secondary plume could be obtained using data from the Stratospheric Aerosol and Gas Experiment III aboard the International Space Station (SAGE III/ISS, hereafter referred to as SAGE). To this end, we present a method of distinguishing between sulfuric acid aerosol and smoke in the stratosphere that uses the SAGE extinction spectra. We discuss limitations of this methodology, namely that it is limited to moderately-sized eruptions (VEI $\leq$5) and large-scale pyroCb events as detailed below.

2 Instrumentation

2.1 SAGE III instrument and data preparation

SAGE is a solar and lunar occultation instrument (Cisewski et al., 2014) that is installed on the ISS and has a data record that began in June 2017. The spectrograph sub-system has a spectral range that extends from 280 to 1040 nm and has a resolution of 1-2 nm. In addition to the spectrograph there is an InGaAs photodiode at 1550 nm. The ISS orbit is inclined at 51.6°, resulting in more observations at midlatitudes than at tropical latitudes as shown by Knepp et al. (2020).

The version 5.2 SAGE data were used in this analysis. The standard products include the number density of gas-phase species for both solar (O_3, NO_2, and H_2O) and lunar (O_3, NO_2, and NO_3) observations, as well as aerosol extinction coefficients (385, 450, 520, 600, 675, 755, 870, 1020, 1550 nm; referenced as k_λ) for solar occultations. The v5.2 release differed from v5.1 in that vertical smoothing for all products, except H_2O, was turned off to provide data at the highest vertical resolution. In this study, the extinction coefficients were filtered to remove data with relative errors in excess of 20% followed by vertical smoothing using a 1-2-1 binomial average to yield a vertical resolution consistent with previous SAGE missions (i.e., 0.75 km, reported every 0.5 km). Finally, the data were limited to altitudes between 2 km above the tropopause (as reported by the Modern-Era Retrospective analysis for Research and Applications, version 2 (MERRA-2) model) and 30 km.

The 520, 600, and 675 nm extinction coefficients had a low bias as demonstrated by Wang et al. (2020) for the v5.1 product, and remains present in the v5.2 product. The bias is more prominent at mid-latitudes and altitudes between 20 and 25 km, and

https://doi.org/10.5194/amt-2021-333
Preprint. Discussion started: 20 October 2021


Atmospheric Measurement Techniques Discussions

is likely the product of ozone interference in the retrieval algorithm. Therefore, k_{520} was replaced by applying an Ångström (power law) correction as described by Eq. (2) where k is the extinction coefficient at the subscripted wavelength.

$$\log k_{520} = \frac{\log\left(\frac{k_{450}}{k_{755}}\right) \cdot \log\left(\frac{520}{755}\right)}{\log\left(\frac{450}{755}\right)} + \log k_{755} \tag{2}$$

2.2 CALIOP

The Cloud-Aerosol Lidar with Orthogonal Polarization (CALIOP) instrument is a space-borne elastic backscatter lidar that has been orbiting the earth in the A-train constellation since 2006 (Winker et al., 2010). In September 2018 the orbit was lowered by 16.5 km to correspond to the orbit of CloudSat which. The onboard Nd:YAG laser emits polarized radiation at 1064 nm and 532 nm. The total backscatter at 1064 nm and both parallel and perpendicular backscatter at 532 nm provides information on the size and shape of the scattering particles. We used data from the version 4.2 product, which has improved calibration particularly suitable for stratospheric studies (Kar et al., 2018; Getzewich et al., 2018; Kim et al., 2018). We also used the level 3 stratospheric aerosol product, which provides aerosol extinction and attenuated scattering ratios in the stratosphere at 5°(latitude), 20°(longitude), and 900 m (vertical) resolution (Kar et al., 2019).

3 The Raikoke plumes

The 22-June, 2019 eruption of Raikoke was rated a VEI-4 that injected SO_2 and ash directly into the stratosphere (between 13 and 19 km). The SAGE instrument observed enhanced extinction layers within one week of the eruption (Fig. 1). The immediate increase in extinction was ≈8-9 times the background conditions, and the stratosphere remained in a non-background state throughout the remainder of 2019 and into 2020. Figure 2 shows the monthly zonal mean extinction coefficient at 1550 nm (k_{1550}) and extinction ratio between the 520 nm and 1550 nm channels ($k_{520} : k_{1550}$) from SAGE as well as the attenuated scattering ratio from CALIOP. The progression of enhanced extinction is seen in panels a-f of Fig. 2. Beginning in July, the extinction coefficient increased between 11 and 13 km and is attributed to Raikoke. No significant enhancement was observed in June because these figures present monthly zonal means and the eruption occurred late in the month, effectively averaging out any enhancement that was detected in the SAGE data. Subsequent months showed significant enhancement as well as how this enhanced layer was transported southward, which is better seen in the extinction ratio plots (panels g-l) and attenuated scattering ratio from CALIOP (panels m-r).

What stood out in Fig. 2, panel (d), was the presence of an enhanced layer at ≈23 km. The initial ascent of this "secondary plume" might be seen as early as August (c) and remained visible in the extinction coefficient plots for the remainder of the year. The extinction ratio plots (panels g-r) as well as the attenuated scattering ratio plots (panels m-r) more readily show the persistence of this layer through November. Historically, extinction ratios have used the 1020 nm channel as reference. However, here we used the 1550 nm channel as reference because this enhanced the contrast between the enhanced layers and background, resulting in a more prominent contrast. It is because of this heightened contrast that the 1550 nm channel was used for reference throughout the remainder of this analysis.

https://doi.org/10.5194/amt-2021-333
Preprint. Discussion started: 20 October 2021

Atmospheric Measurement Techniques Discussions

A possible reason for the lofting of this layer could be diabatic heating as has been demonstrated for smoke in previous wildfires (Boers et al., 2010; de Laat et al., 2012; Yu et al., 2019). Per this hypothesis, as the Sun shone through this portion of atmosphere, particles within the secondary plume absorbed the incoming solar radiation, which resulted in the air mass heating, thereby decreasing its density, which resulted in further lofting until equilibrium was reached. Though this scenario is not unreasonable for an absorbing aerosol, this is unexpected behavior for weakly-absorbing species like sulfuric acid aerosol and is generally not observed in association with the mid and high-latitude eruptions of the past. Below 2 μm, the imaginary component of sulfuric acid's refractive index is effectively zero (i.e., $\ll$1E-5; Palmer and Williams (1975)), precluding the level of absorption required for subsequent heating/lofting. However, this behavior would be consistent with absorbing particles typically found in smoke from biomass burning events that occasionally inject black and brown carbon directly into the stratosphere during pyroCb events. Therefore, we hypothesized that smoke was present in the stratosphere during the Raikoke eruption and that this smoke layer lofted up to $\approx$25 km as it circulated the globe and migrated southward as demonstrated in Chouza et al. (2020).

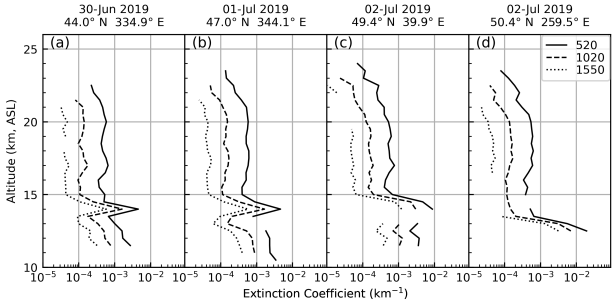

Figure 1. SAGE extinction coefficient profiles at 3 wavelengths showing the Raikoke plume between 12 and 14 km.

4 Evaluation of smoke and sulfuric acid extinction spectra from Mie theory

In order for the ascending air mass to be diabatically heated there must be an absorbing species present and we hypothesized that this absorbing species is black and brown carbon found in smoke from coincident wildfires in Siberia and western Canada. While the composition and spectral characteristics of smoke are highly variable (Bergstrom et al., 2002; Müller et al., 2005; Park et al., 2018; Kozlov et al., 2014; Womack et al., 2021), there is commonality between burning events in that the real component of the refractive index is spectrally flat and the imaginary component is variable (both behaviors being significantly different from sulfuric acid aerosol). Therefore, it is reasonable that the extinction spectra (extinction coefficients or extinction ratios as a function of wavelength) for smoke and sulfuric acid aerosols would differ significantly and that this difference may be useful in distinguishing between the two aerosol types.

As an initial test of this hypothesis we used Mie theory to calculate extinction coefficients at SAGE wavelengths for sulfuric acid aerosol and smoke. The primary challenge in carrying out this simulation is the highly-variable nature of smoke's refractive

https://doi.org/10.5194/amt-2021-333
Preprint. Discussion started: 20 October 2021

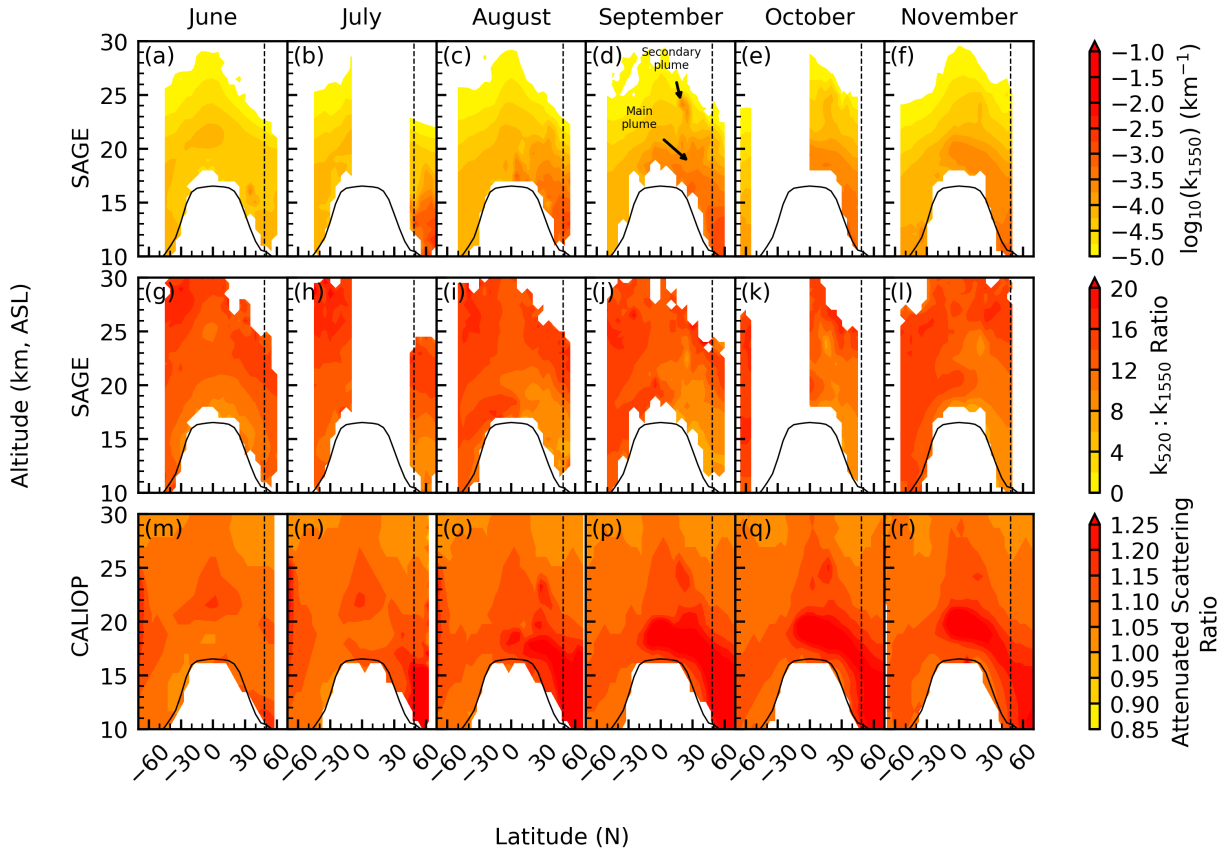

Figure 2. Zonal monthly mean of 1550 nm extinction coefficients (panels a-f), 520:1550 extinction ratio (panels g-l), and attenuated scattering ratio from CALIOP (panels m-r). The solid black line indicates the average tropopause altitude and the dashed black line indicates Raikoke's latitude.

index, which is dependent on fuel source, burn temperature, humidity, age, etc. Further, smoke in the stratosphere is aged and its composition has likely changed during its transport due to ongoing chemistry (Yu et al., 2019). Therefore, the likelihood of this smoke's refractive index being consistent with the refractive index measured from aircraft or laboratory settings is small. To our knowledge there have been no refractive index measurements for stratospheric smoke. Therefore, we used two sets of smoke refractive indices to span the range of reasonable refractive index values. The Bergstrom et al. (2002) refractive indices are representative of black carbon (BC) that comes from complete combustion, and the Sumlin et al. (2018) refractive indices are representative of brown carbon (BrC) smoke from biomass burning events (see Table 1 for values). While it is unlikely that stratospheric smoke is composed of BC and is more likely composed of BrC, this selection of refractive indices provides reasonable bounds, covering all potential values, within this simulation.

https://doi.org/10.5194/amt-2021-333
Preprint. Discussion started: 20 October 2021


Atmospheric Measurement Techniques Discussions

The simulation consisted of two parts: 1. assume a lognormal distribution with constant mode radius (200 nm) and distribution width (1.5) to visualize the expected extinction spectrum; 2. assume a lognormal distribution with constant distribution width (1.5) and variable mode radius (40–500 nm) to visualize how the slopes changed as a function of particle size. The results of this simulation are presented in Fig. 3 wherein it is observed that the two species have different spectral behavior for extinction coefficients (panel a) and that the slopes were consistently different for small particle sizes. We emphasize that this model is very simple, contains multiple assumptions, and presents a general relationship that is in no way intended to be representative of actual conditions. Certainly, changing the smoke refractive indices from BC to BrC values significantly changed the extinction spectrum as well as the spectral slopes with the BrC slopes remaining significantly different from sulfuric acid (≈2x smaller). However, the model remains robust as a general guide for providing a testable hypothesis. While the details of the size distribution, refractive indices, and number densities can modulate the differences in the slope, this has no impact on the subsequent analysis. Finally, we note that, as shown in panel (b) of Fig. 3, when particle sizes become large the slopes become less distinguishable because of the convergence of extinction coefficients at large particle sizes (as demonstrated by Thomason (1992) and Thomason et al. (2008) using extinction ratios). The consequence of this is that the current method is not applicable to large eruptions, such as the 1991 eruption of Mt. Pinatubo, which result in the formation of large sulfuric acid particles. The intent of this simulation is solely to demonstrate that smoke will have flatter spectra than sulfuric acid aerosol that is the product of small to moderate volcanic eruptions.

λ (nm)	Sulfuric Acid	BC	BrC
385	1.448 + 0i	1.75 + 0.50i	1.55 + 1.0E-2i
450	1.434 + 0i	1.75 + 0.50i	1.55 + 4.4E-3i
520	1.431 + 0i	1.75 + 0.50i	1.55 + 2.6E-3i
600	1.430 + 6.38E-9i	1.75 + 0.50i	1.55 + 2.0E-2i
675	1.429 + 1.70E-8i	1.75 + 0.50i	1.55 + 2.0E-2i
755	1.427 + 7.59E-8i	1.75 + 0.65i	1.55 + 2.0E-2i
870	1.425 + 1.91E-7i	1.75 + 0.65i	1.55 + 2.0E-2i
1020	1.421 + 1.51E-6i	1.75 + 0.75i	1.55 + 2.0E-2i
1550	1.403 + 1.42E-4i	1.75 + 0.90i	1.55 + 2.0E-2i

Table 1. Complex refractive indices for smoke and sulfuric acid used in the Mie simulations. The smoke refractive index values were based on data collected by Bergstrom et al. (2002) for BC and Sumlin et al. (2018) for BrC. Sulfuric acid refractive index values are from Palmer and Williams (1975).

What stood out most in this simulation was the stark contrast between the sulfuric acid and smoke aerosol types; i.e., the difference in how rapidly the extinction coefficients changed with wavelength. Indeed, the sulfuric acid values changed more rapidly than those for smoke, indicating that, when sulfuric acid aerosol is the predominant aerosol type, the overall slope of the extinction spectrum will be much larger (i.e., more negative) than when the atmosphere is laden with smoke. This distinction

https://doi.org/10.5194/amt-2021-333
Preprint. Discussion started: 20 October 2021

Atmospheric Measurement Techniques Discussions

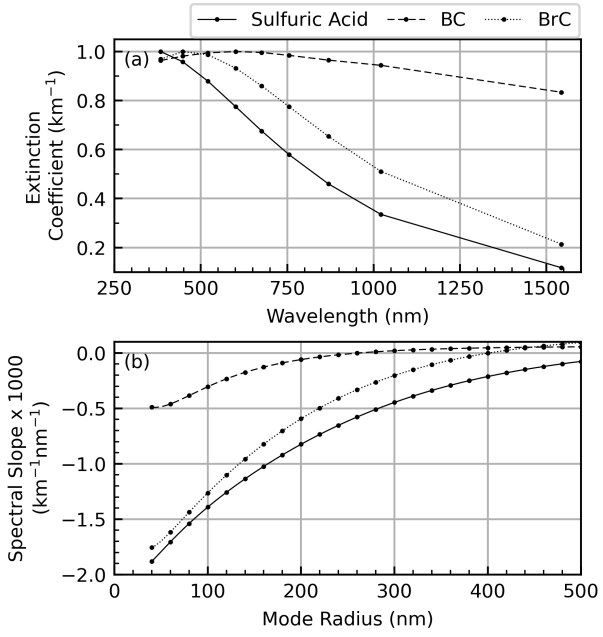

Figure 3. Spectra of extinction coefficients (normalized to 1) as a function of wavelength (a) and spectral slope as a function of mode radius (b) from the Mie theory simulation.

provides a testable hypothesis to determine, preliminarily, the viability of separating smoke and sulfuric acid aerosol in real-world data. To this end, data collected during the four case-study events listed in Table 2 were used to see, broadly speaking, whether the different events showed consistent spectral differences. Data were selected for each event by truncating the data record to include profiles collected within $\pm 5^\circ$ latitude of the event, and included data collected one month prior to, and three months after, the event (a four-month window) from 14–25 km. The extinction ratios (a proxy for spectral slope) for these four events are presented as a function of k_{1020} in Fig. 4.

Similar to the theoretical work (Fig. 3), the two volcanic events in the SAGE data (Fig. 4, panels a and b) showed very different behavior from the wildfire events (panels c and d). On one hand, as k_{1020} increased for the volcanic events the extinction ratio increased slightly, though it remained mostly unchanged, suggesting that both the composition and mean size of the optically important aerosol has remained unchanged from background (following Thomason et al. (2021)). On the other hand, the extinction ratios for the wildfire events had distinctly different behavior, quickly merging to smaller values (<10) as the extinction coefficient increased. This figure demonstrates that the measured extinction ratios behave as expected from the model and that, at least preliminarily, the two event types can be distinguished.

At this point we must reiterate the caveat that this holds true only for small or moderate eruptions and would not be applicable to larger eruptions such as the 1991 eruption of Mt. Pinatubo. Eruptions that inject large amounts of SO_2 into the stratosphere, like Pinatubo, have been observed to rapidly produce extinction ratios indistinguishable from water clouds and presumably

https://doi.org/10.5194/amt-2021-333
Preprint. Discussion started: 20 October 2021


Atmospheric Measurement Techniques Discussions

smoke. This process involves the conversion of SO_2 to gaseous sulfuric acid (e-folding time of ≈30 days) which then either deposits on to existing aerosol or nucleates to form many small particles that coagulate to form optically large aerosol. Indeed, the first SAGE II observations of the main Pinatubo plume (when transmission was not saturated) showed a 525 to 1020 nm extinction coefficient ratio of essentially 1 (Thomason, 1992). However, within the framework of the current study we only consider relatively smaller eruptions that inject much less SO_2 into the stratosphere, with Raikoke (VEI-4) being the largest.

Up to now we have only considered the raw extinction spectrum (e.g., Fig. 3 (a)) and a simple combination of extinction coefficients expressed as the extinction ratio (Fig. 4). This was useful for comparing measurements to theory and for providing rudimentary visualizations, though it requires the analysis to be done on a channel-by-channel or extinction ratio-by-extinction ratio basis (hence the three colors in Fig. 4). Indeed, using a single extinction ratio (e.g., $k_{520} : k_{1020}$) yielded results that were similar to the spectral-slope approach. However, all of the information in these four ratios can be efficiently combined into a single number within the spectral slope, thereby eliminating the channel-by-channel approach, streamlining the analysis, mitigating the potential for noise in a single channel to influence the outcome, as well as mitigating the impact of the low bias in the k_{520} channel. Therefore, given the consistent behavior between the model and the measured extinction ratios we hypothesize that small-to-moderate volcanic eruptions that inject material into the stratosphere can be distinguished from wildfire events in the SAGE record by looking at the spectral slope.

Event	Date	Altitude (km)	Latitude
Canadian wildfire	August 2017	14-25	52°N
Ambae eruption	April/July 2018	14-25	15°S
Raikoke mixed	June 2019	14-25	48°N
Ulawun eruption	June/August 2019	14-25	5°S
Australia wildfire	January 2020	14-25	35°S

Table 2. Listing of major events used in the current study. The Raikoke event is labeled as a mixed type because of the impact of coincident wildfires in Siberia and western Canada. The altitude column refers to the altitude range used in creating Fig. 4.

5 Detection and classification method

To test the aforementioned hypothesis, we evaluated the change in spectral slope as a function of k_{1020} for 4 case-study events (2 pyroCb, 2 volcanic; see §6 for details). To do this, the spectral slope was calculated via linear regression where channel wavelength (nm) acted as the independent variable and $\log_{10}(\boldsymbol{k})$ was the dependent variable. The 385 channel was excluded from this analysis because of its rapid attenuation at relatively high altitudes (≈18 km). The 600 and 675 nm channels were excluded from the linear regression due to the impact ozone has on these aerosol channels. Further, to reduce the influence of potentially spurious measurements, a conservative cutoff was applied by excluding all extinction coefficients that had relative error >20% and we only used extinction spectra that had valid values in the 6 remaining channels (450, 520, 755, 870, 1020,

https://doi.org/10.5194/amt-2021-333
Preprint. Discussion started: 20 October 2021

Atmospheric Measurement Techniques Discussions

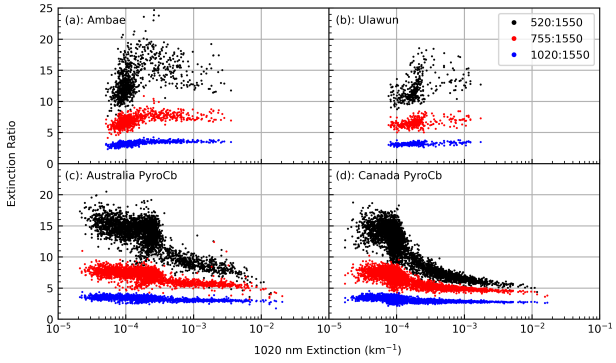

Figure 4. Extinction ratio plots, using 3 ratios, for the four case study events. All ratios were referenced to the 1550 nm channel.

1550 nm). These slopes were evaluated for each case study event and the results were then applied to the Raikoke event to distinguish between sulfuric acid aerosol and smoke within this single event (see §7).

Not all profiles collected after a volcanic or wildfire event were impacted by that event. Therefore, a method for discriminating between background and perturbed conditions was developed. The use of median ($\tilde{X}$) and median absolute deviation (MAD) has become a popular, statistically robust, alternative to using mean and standard deviation for the elimination of outliers and their impact on an analysis (Leys et al., 2013). If the sample population is normally distributed, then MAD · 1.4826 is equivalent to 1 standard deviation (1-σ). Therefore, we implemented a more rigorous definition of MAD (labeled MAD*, $\approxeq$ 2-σ) as defined in Eq. (3) where $b = 2 \cdot 1.4826$ and $\boldsymbol{x}$ is an array of the dataset under investigation.

$$\text{MAD}^* = b \cdot \text{median}(|\boldsymbol{x} - \tilde{X}|) \tag{3}$$

Herein, the median and MAD* of the spectral slopes ($\tilde{X}_m$, MAD$^*_m$) and k_{1020} ($\tilde{X}_k$, MAD$^*_k$) collected during background periods were calculated for each event, as a function of altitude, using data collected within 5°of the each event's latitude. Initially, the background statistics were calculated using only the month prior to each event, but that provided insufficient sampling for the Ambae and Ulawun events due to SAGE's observation schedule (see, for example, Fig. 1 of Knepp et al. (2020)). Therefore, the background time period for the Ambae and Ulawun events was expanded to include 9 months prior to the eruption. The Ulawun eruption required an additional modification. Ambae and Ulawun are geographically close (≈2000 km) and Ulawun erupted within a year of Ambae's last eruption. Therefore, the stratosphere was still recovering in the months prior to the Ulawun eruption, which biased the background statistics. Background statistics for Ulawun were calculated using profiles collected in Ulawun's latitude band (±5°), but using data collected in the 9 months leading up to the Ambae eruption.

Spectra were assigned one of 3 classifications based on the following criteria (here, $\tilde{X}$ and MAD* refer to background conditions):

1. **Background:** When extinction was not enhanced. i.e.,

$$k_{1020} \leq \tilde{X}_k + \text{MAD}^*_k$$

https://doi.org/10.5194/amt-2021-333
Preprint. Discussion started: 20 October 2021


Atmospheric Measurement Techniques Discussions

2. **Sulfuric acid aerosol:** When extinction was enhanced, and the slope was less than (i.e., more negative) or equal to the background slope.

$$(k_{1020} > \tilde{X}_k + \text{MAD}_k^*) \ \& \ (\text{slope} \leq \tilde{X}_m + \text{MAD}_m^*)$$

3. **Smoke:** When extinction was enhanced and the slope was flatter than background conditions.

$$(k_{1020} > \tilde{X}_k + \text{MAD}_k^*) \ \& \ (\text{slope} > \tilde{X}_m + \text{MAD}_m^*)$$

A shortcoming of this classification scheme is that it uses hard cutoff values to separate the aerosol types while, in reality, particles near the smoke/sulfuric acid cutoff would likely be a mixture of the two and not strictly homogeneous. However, the utility of this method, as described, makes the identification of smoke highly conservative.

5.1 Layer identification with CALIOP

Ideally, this characterization scheme would be validated with in situ sampling of the various and disparate aerosol layers, which requires expansive sampling on a global (or at least a hemispherical) scale that is not feasible. However, the CALIOP lidar has polarization sensitivity at 532 nm which can be used to make general composition estimates (e.g., sulfuric acid aerosol, smoke, dust, cloud, and volcanic ash). Smoke injected into the stratosphere due to pyroCb events can be discriminated from sulfuric acid aerosol based on the level of depolarization in the return signal (Kim et al., 2018). The ratio of the perpendicular and parallel polarized components of the backscatter (depolarization ratio), provides information about the shape of the scattering particles. In general, the depolarization ratio of tropospheric smoke is quite low (<0.05). However, the depolarization ratio of smoke detected in the stratosphere from pyroCb events have much higher depolarization ratio (0.1-0.2, per Christian et al. (2020)). This feature can be used to separate stratospheric smoke from the volcanic sulfate particles which are spherical and thus do not depolarize. In addition to depolarization ratio, the CALIOP data products contain a vertical feature mask (VFM) product that classifies the different types of detected layers as aerosol (tropospheric and stratospheric) and clouds (Vaughan et al., 2018). Both depolarization ratio and the VFM were used herein to corroborate the identification of sulfuric acid aerosol and smoke within the SAGE data.

6 Application to case studies events

In this study we considered five events that had significant impact on the stratosphere as detailed in Table 2. Excluding Raikoke, these events were classified as either primarily volcanic or wildfire related, which provides four test cases for evaluating distinct behaviors for each event class. While the majority of the data collected for these events appears to come from a single source, we add the caveat that some events were close enough in time and geography to experience some carryover (e.g., the two Ulawun eruptions and the Australian pyroCb), which will be briefly discussed below.

To better appreciate the finer details of the profile data, and to demonstrate which parts of the atmosphere were most impacted by each event, the data were broken into 1 km bins. Statistics for labeling the different layer types in the 4 case-study events are

https://doi.org/10.5194/amt-2021-333
Preprint. Discussion started: 20 October 2021

Atmospheric Measurement Techniques Discussions

presented in Table 3, which contains the total number of valid spectra collected at each altitude, the number of non-background spectra identified using the above cutoff criteria, and the fraction of enhanced spectra identified as either smoke or sulfuric acid aerosol.

		Altitude (km)											
		14	15	16	17	18	19	20	21	22	23	24	25
Ambae	Total Spectra	4	15	41	148	628	1391	1583	1586	1586	1586	1586	1586
	Enhanced Layers	0	3	17	51	249	479	479	339	189	48	8	0
	Sulfuric Acid	—	1.0	1.0	1.0	1.0	1.0	1.0	1.0	0.97	0.69	0.38	—
	Smoke	—	—	0	0	0	0	0	0	0.03	0.31	0.62	—
Ulawun	Total Spectra	0	1	2	29	205	755	889	892	892	892	892	892
	Enhanced Layers	0	1	2	18	154	627	867	883	855	704	395	34
	Sulfuric Acid	—	0	1.0	0.89	0.97	1.0	1.0	1.0	1.0	1.0	1.0	1.0
	Smoke	—	1.0	0	0.11	0.03	0	0	0	0	0	0	0
Canada	Total Spectra	2690	3194	3386	3546	3706	3794	3800	3800	3800	3800	3800	3800
	Enhanced Layers	2204	2669	2868	2957	2916	2808	2298	1689	1254	1267	1327	1217
	Sulfuric Acid	0.62	0.27	0.20	0.19	0.16	0.20	0.12	0.13	0.26	0.57	0.90	0.99
	Smoke	0.38	0.73	0.80	0.81	0.84	0.80	0.88	0.87	0.74	0.43	0.10	0.01
Australia	Total Spectra	3402	3789	3935	4029	4113	4135	4138	4138	4138	4138	4138	4138
	Enhanced Layers	2472	2885	3080	3204	3218	3142	2885	2710	2620	2441	2172	1865
	Sulfuric Acid	0.01	0.01	0	0.01	0.04	0.06	0.06	0.06	0.09	0.14	0.14	0.30
	Smoke	0.99	1.0	1.0	0.99	0.96	0.94	0.94	0.94	0.91	0.86	0.86	0.60
Raikoke Primary	Total Spectra	1231	1483	1590	1631	1646	1652	1652	1652	1652	1652	1652	1652
	Enhanced Layers	969	1166	1236	1211	1078	753	329	344	389	387	261	123
	Sulfuric Acid	0.11	0.26	0.34	0.26	0.25	0.16	0.11	0.20	0.35	0.91	0.95	0.96
	Smoke	0.89	0.74	0.66	0.74	0.75	0.84	0.89	0.80	0.65	0.09	0.05	0.04
Raikoke Secondary	Total Spectra	10	32	69	185	458	812	896	896	896	896	896	896
	Enhanced Layers	10	28	54	127	319	484	471	380	60	108	218	125
	Sulfuric Acid	0	0.5	0.56	0.65	0.70	0.71	0.69	0.72	0.20	0.02	0.33	0.70
	Smoke	1.0	0.5	0.44	0.35	0.30	0.29	0.31	0.28	0.80	0.98	0.67	0.30

Table 3. Layer classification statistics from SAGE data. Total number of valid spectra, total number of identified layers as well as the fraction of spectra identified as smoke or sulfuric acid aerosol for each case-study event.

https://doi.org/10.5194/amt-2021-333
Preprint. Discussion started: 20 October 2021


Atmospheric Measurement Techniques Discussions

6.1 Volcanic events

The classification scheme worked well for both volcanic case-study events as there were only 34 spectra mis-classified as smoke (out of >6400, ≈0.5%). It was observed that as extinction increased, the slopes tended to remain approximately consistent with background slopes, or became slightly more negative as seen in Figs. 5 and 6. Overall, there was little deviation from background conditions other than the enhanced extinction. This limited change in slope is reasonable because background stratospheric aerosol is composed of primarily sulfuric acid and the injection of SO_2 from moderately-sized volcanic events led to further formation of sulfuric acid aerosol. While this increased the overall extinction coefficient, its impact on the spectral slope was minimal due to the consistent composition and hence spectral properties under background and elevated loads.

We note that the Ulawun event had a small number of points that were classified as smoke with elevated k_{1020} between 17 and 18 km. While it is not unreasonable to have misclassifications, we note that these spectra were collected in January and February 2020, at the peak of the Australian wildfire, when smoke had transported over the Ulawun latitude range (Kloss et al., 2021). While we cannot definitively attribute these data points to smoke from the Australia pyroCb, the general pattern observed here (slope rapidly approached 0 with increasing extinction) is consistent with what was observed for the pyroCb events (*vide infra*) and we note this as interesting.

Though evidence for ash in the stratosphere, for these events, is tenuous, we cannot categorically exclude the possibility that ash was present in the stratosphere for at least part of each event's time period. However, if ash were present, it would result in more spectra being classified as smoke because, as discussed above, large particles tend to flatten the extinction spectra while enhancing k as was seen during Pinatubo. Indeed, this may be the cause of some of the smoke classifications in the Ulawun event mentioned above. However, particles of this size are not expected from these moderately-sized eruptions. Therefore, we conclude that ash and any other potentially large aerosol (sulfuric acid) do not appreciably impact the optical measurements and that the majority of slopes presented in Figs. 5, 6 are reflective of small sulfuric acid aerosol only.

Figures 7 and 8 show examples of the CALIOP depolarization ratio (panel a), the CALIOP VFM (panel b), SAGE extinction profiles (panel c) as well as the SAGE spectral slope profile (panel d) for Ambae and Ulawun, respectively. The figure title provides the SAGE overpass date, latitude, longitude, and distance to the nearest CALIOP profile. The vertical arrow above panel (a) indicates the location of the SAGE overpass relative to the CALIOP curtain plot.

For both events, the peak in extinction corresponded well with a rapid decrease in spectral slope (i.e., became more negative) and a stratospheric aerosol layer identified in the CALIOP VFM between 17 and 19 km, and no significant depolarization, giving credence to the SAGE-based identification scheme for sulfuric acid aerosol.

6.2 Wildfire events

The wildfire events showed a mix of classifications, though the classification became uniformly smoke with increasing k_{1020}, as shown in Figs. 9 & 10. Further, as compared to background conditions, the slopes changed by up to 80%. The lowermost altitudes for the Australia events showed a nearly monolithic identification of smoke, as well as a distinct separation from

https://doi.org/10.5194/amt-2021-333
Preprint. Discussion started: 20 October 2021

Atmospheric Measurement Techniques Discussions

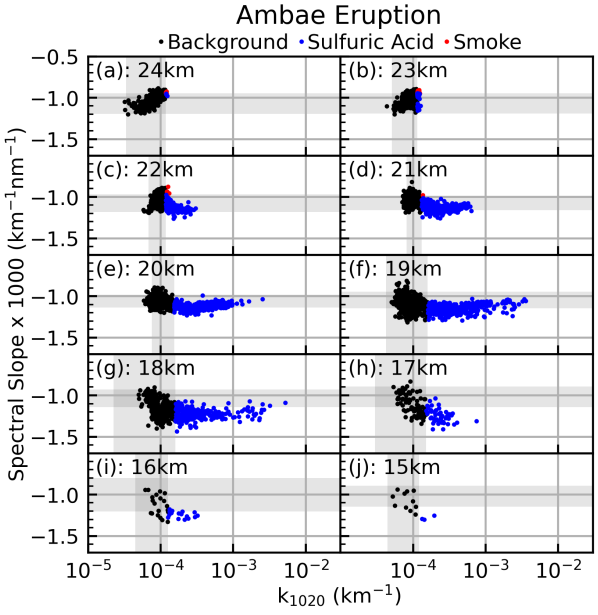

Figure 5. Spectral slope (x1000) as a function of k_{1020} and altitude for data collected over the Ambae eruption. The gray shaded regions indicate the width of MAD* as described in Eq. (3).

background conditions, which makes sense since the lowermost altitudes are the most impacted by these events. The Canadian wildfire likewise showed a nearly uniform identification of smoke.

While the volcanic events showed nearly uniform identification of sulfuric acid aerosol under elevated conditions, the wildfire events showed a significant portion of the spectra identified as sulfuric acid aerosol (≈10,000 out of >58,000; ≈19%). Of these ≈10,000 sulfuric acid classifications, ≈48% of them were in the Canadian wildfire event between 23 and 25 km. The reason for the presence of elevated sulfuric acid aerosol within the wildfire events could be for two reasons. First, within the current identification scheme, it is possible for smoke to be identified as sulfuric acid because of the combination of the SAGE viewing geometry and the optical thinness of parts of the smoke plume (i.e., depending on whether SAGE is sampling through the centroid of the plume or only the outer edge). It is reasonable that, when sampling optically thin smoke layers, the extinction will be elevated above background levels, but the slope may not deviate significantly. This can be achieved when the viewing geometry is such that only optically thin portions of the smoke plume are sampled, thereby raising the extinction coefficients, but the overall, integrated aerosol along the viewing path is not sufficiently different from background conditions to significantly change the spectral slope. This could lead to an ambiguous characterization of aerosol composition at extinctions that are outside background values, but still at the lower end of extinction values for that particular event as seen in Figs. 9 & 10. This scenario is the most likely and is expected from a statistical viewpoint. Secondly, a less likely scenario is there may be elevated levels of sulfuric acid aerosol within the sampling volume due to transport from a nearby volcanic event. Indeed, this may be the case for some of the spectra classified as sulfuric acid in the Australian wildfire case study. In contrast to the Canadian

https://doi.org/10.5194/amt-2021-333
Preprint. Discussion started: 20 October 2021

Atmospheric Measurement Techniques Discussions

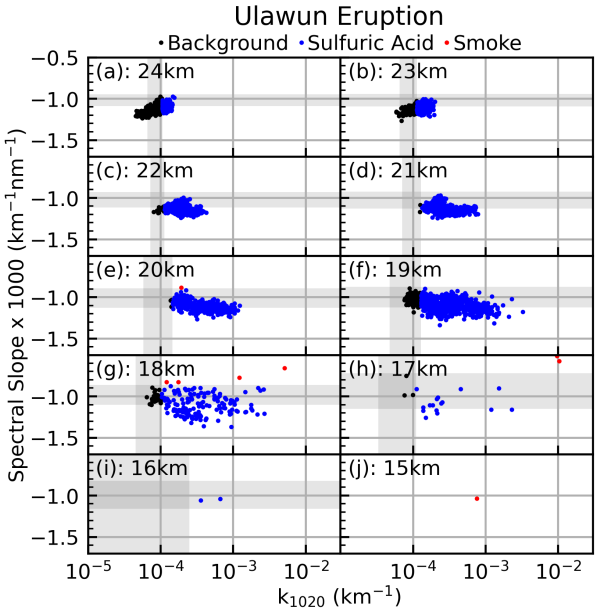

Figure 6. Same as Fig. 5, but for the Ulawun eruption.

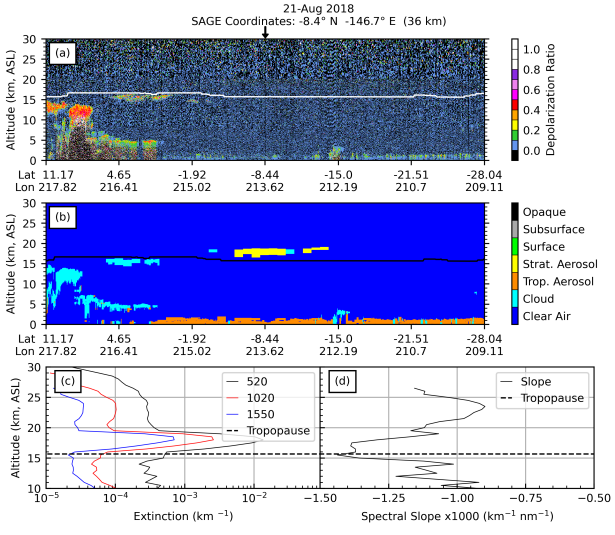

Figure 7. CALIOP and SAGE data collected during the Ambae eruption. The title indicates the date, SAGE overpass coordinates, and the distance between the SAGE profile and the nearest CALIOP profile. The vertical arrow above panel (a) indicates the location of the SAGE profile along the CALIOP flight path. Solid horizontal lines (panels a and b) indicate tropopause altitude.

https://doi.org/10.5194/amt-2021-333
Preprint. Discussion started: 20 October 2021

Atmospheric Measurement Techniques Discussions

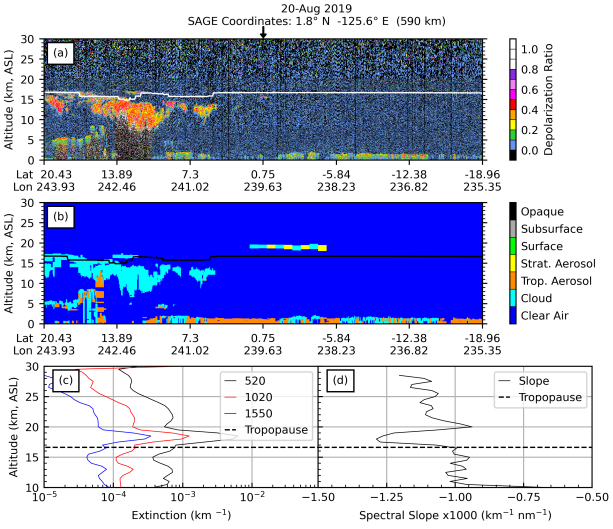

Figure 8. Same as Fig. 7, but for the Ulawun eruption.

wildfire, the range of background extinction coefficients for the Australian fire spanned a wider range and extended into higher extinction coefficients (e.g., >5E-4 at 16 km), indicating the apparent background conditions were perturbed, potentially from the 2019 Ulawun eruptions (Kloss et al., 2021). Regardless of why spectra were classified as sulfuric acid, the performance of this identification scheme remains encouraging as the majority (>81%) of non-background values were identified as smoke within these layers as shown in Table 3. Further, the distribution of data for the wildfire events is markedly different from the volcanic events, indicating that we are observing two distinctly different aerosol types.

Figures 11 and 12 show examples of the CALIOP and SAGE profile data collected over the two wildfire case-study events. Here, CALIOP showed significant depolarization near 19 km (Canadian pyroCb) and 14 km (Australian pyroCb), which corresponded well with a rapid increase in both aerosol extinction and spectral slope in the SAGE profile data. We note that in Fig. 12 SAGE saw another layer at 19 km that was not manifest within the CALIOP VFM or depolarization ratio profiles. This altitude is well within the SAGE instrument's operational altitude range and may be reflective of the relatively poor return signal at this altitude for CALIOP and its narrow swath width. Alternatively, SAGE may have sampled a narrow smoke filament that was not within the CALIOP sample volume.

Overall, the CALIOP data products provided good support for the SAGE-based classification of stratospheric aerosol composition. Therefore, this identification scheme will now be applied to a much more heterogeneous event: the 2019 Raikoke eruption.

https://doi.org/10.5194/amt-2021-333
Preprint. Discussion started: 20 October 2021

Atmospheric Measurement Techniques Discussions

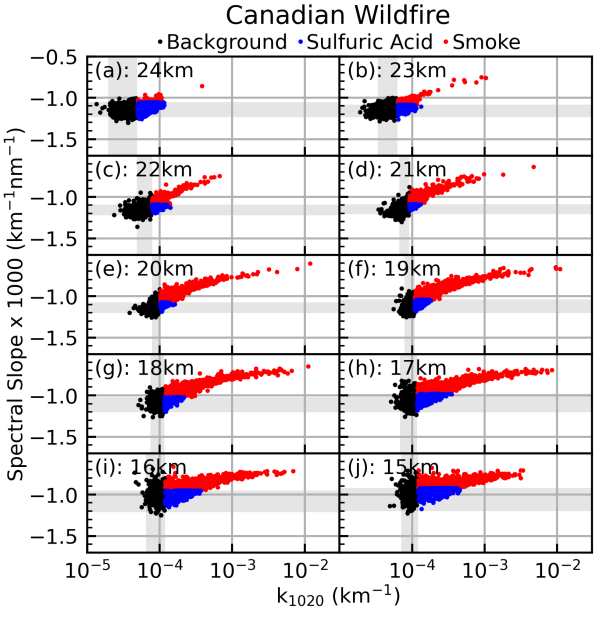

Figure 9. Same as Fig. 5, but for the Canadian wildfire.

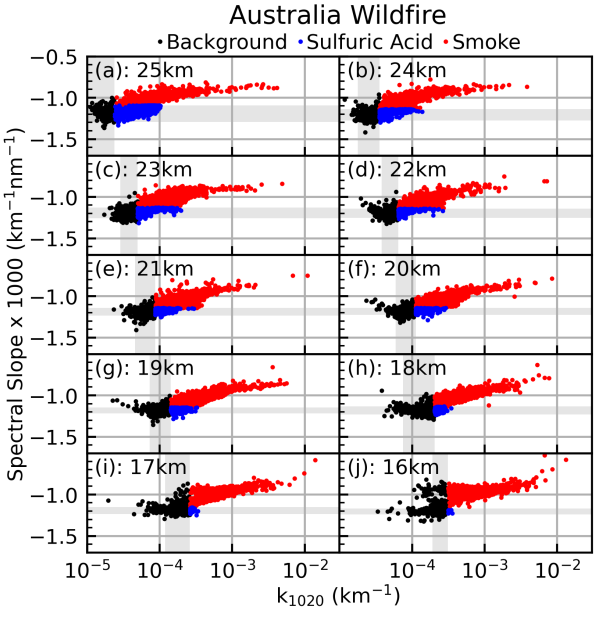

Figure 10. Same as Fig. 5, but for the Australian wildfire.

https://doi.org/10.5194/amt-2021-333
Preprint. Discussion started: 20 October 2021

Atmospheric Measurement Techniques Discussions

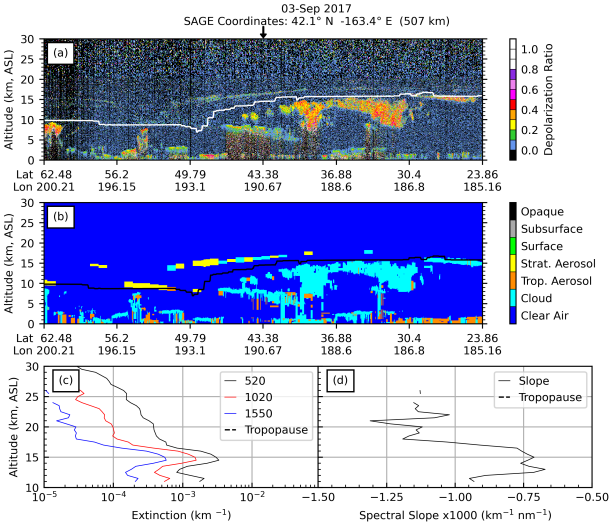

Figure 11. Same as Fig. 7, but for the Canadian pyroCb.

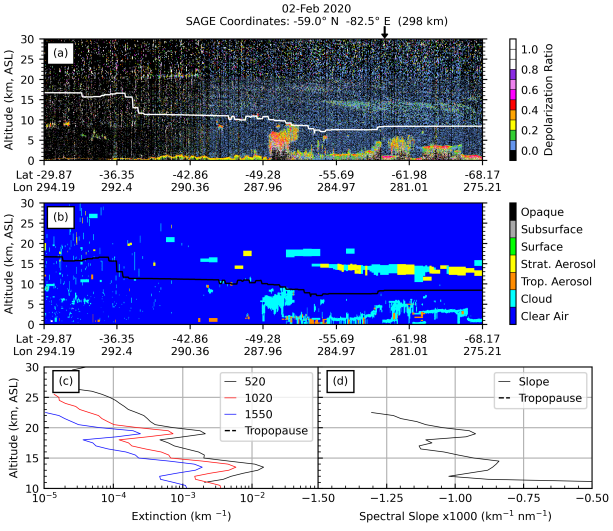

Figure 12. Same as Fig. 7, but for the Australia pyroCb.

7 Application to the Raikoke event

7.1 Smoke present in stratosphere prior to Raikoke

Though there were two pyroCb events in the northern hemisphere during the summer of 2019 (Siberia and western Canada per Kloss et al. (2021) and Vaughan et al. (2021)), there were no wildfire events of similar magnitude as the 2017 Canadian

https://doi.org/10.5194/amt-2021-333
Preprint. Discussion started: 20 October 2021

Atmospheric Measurement Techniques Discussions

wildfire or the 2020 Australian burn. However, Vaughan et al. (2021) claimed they may have observed stratospheric smoke prior to the Raikoke eruption, Kloss et al. (2021) suggested the NH wildfires impacted the stratosphere, and Bachmeier, Scott (2019) classified the Siberian wildfire near Lake Bolon as a pyroCb. Similarly, we applied our method to identify an unambiguous smoke signal in the stratosphere prior to, or immediately coincident with, the Raikoke eruption. To this end, we evaluated SAGE and CALIOP data collected to the west of Raikoke (i.e., upwind, see Fig. 13). Unfortunately, SAGE did not begin sampling this latitude band until after the eruption, therefore we limited our analysis to the first two weeks after the eruption and to a region far enough west of Raikoke to not have been impacted by the volcanic ejecta.

Both SAGE and CALIOP collected profiles within this region and indicated the presence of smoke at ≈13 km as seen in Fig. 14. These profiles were collected within 8 days of the eruption, while the plume still resided over the North Pacific ocean (Kloss et al., 2021; Vaughan et al., 2021). This enhancement was most noticeable in the CALIOP data as well as the spectral slope profile. Indeed, the spectral slope shows a sharp gradient at this altitude, before returning to background conditions between 15 and 20 km (compare to background conditions during the 2017 Canadian pyroCb event, Fig. 11), while the CALIOP depolarization ratio and VFM showed a distinct layer between 10 and 15 km. Therefore, while the SAGE sampling schedule did not allow us to evaluate profiles collected prior to this time, this smoke layer was persistent over this region, in both the SAGE and CALIOP records, throughout the first ≈2 weeks after the eruption and we concur with previous authors that smoke was present in the stratosphere during this time period and was visible in both the SAGE and CALIOP profiles.

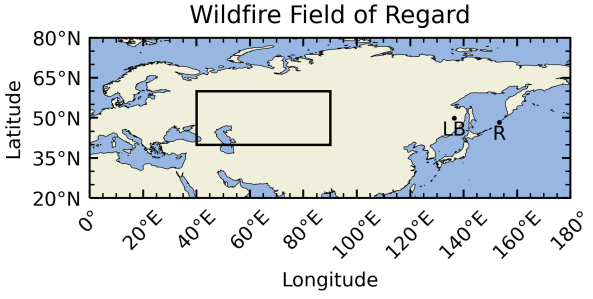

Figure 13. Field of regard for sampling air that has not been impacted by the Raikoke event, but may have been impacted by coincident NH wildfires. LB and R indicate location of the Lake Bolon, Siberia fire and Raikoke, respectively.

7.2 Raikoke main peak

As stated in the introduction, Raikoke erupted on 22-June 2019 and injected SO_2 and ash directly into the stratosphere, at around 15 km altitude, and was observed by SAGE approximately one week later (Fig. 1). Immediately after the eruption, the main Raikoke plume broke into two distinct plumes. One plume moved southward and appeared to be primarily ash as determined by Kloss et al. (2021) and Vaughan et al. (2021). The ash in this plume settled out within a week of the eruption (Kloss et al., 2021). The second plume moved to the north and east and was composed primarily of SO_2 (Kloss et al., 2021), (which was in the process of being converted into sulfuric acid) before getting temporarily trapped within the Aleutian low

https://doi.org/10.5194/amt-2021-333
Preprint. Discussion started: 20 October 2021

Atmospheric Measurement Techniques Discussions

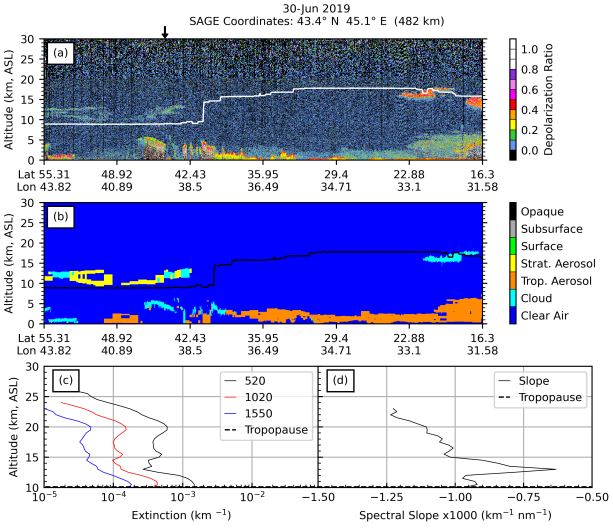

Figure 14. Smoke identified within an air mass that has yet to be impacted by the Raikoke eruption, but was sampled within 8 days of the Raikoke eruption.

(Kloss et al., 2021). This SO_2 plume remained between Kamchatka and Alaska for 2-3 weeks (de Leeuw et al., 2020; Vaughan et al., 2021) before moving eastward over the United States, the UK, and Europe. Therefore, similar to the case-study events, data collected near Raikoke's latitude (48°N, ±5°) and within 7 months after the eruption were used in this analysis. Because of the broad time range and the lack of longitudinal limitations there were a non-negligible number of spectra that fell into the background classification, similar to the case-study events.

Based on the results presented in the previous section, we anticipated that the spectral slopes of the SAGE data collected over the Raikoke event would behave similar to those for Ambae and Ulawun. However, as shown in Fig. 15 and Table 3 the Raikoke data presented what appears to be a mixture of sulfuric acid aerosol and smoke, with the predominant composition being smoke (only 10-30% of spectra were identified as sulfuric acid aerosol). Indeed, the majority of lower-altitude spectra were identified as smoke, while the balance seemed to shift at the highest altitude (23 km). While we anticipated observing smoke within the profiles we did not expect the majority of the spectra to be identified as such. Overall, the Raikoke data look more like a wildfire event than the other volcanic events in this study. Given the magnitude of this eruption, the spectra identified as smoke here may be the product of both ash and large particle formation, both of which have short lifetimes in the stratosphere.

7.3 Interpretation of the secondary Raikoke plume

As shown in Fig. 2, a secondary layer of elevated aerosol broke off from the main Raikoke plume as it moved southward and continued to loft to higher altitudes. The composition of this secondary plume was speculated to contain smoke from NH wildfires, which would cause it to absorb incoming solar radiation, warm the surrounding air, and diabatically loft. This layer

https://doi.org/10.5194/amt-2021-333
Preprint. Discussion started: 20 October 2021

Atmospheric Measurement Techniques Discussions

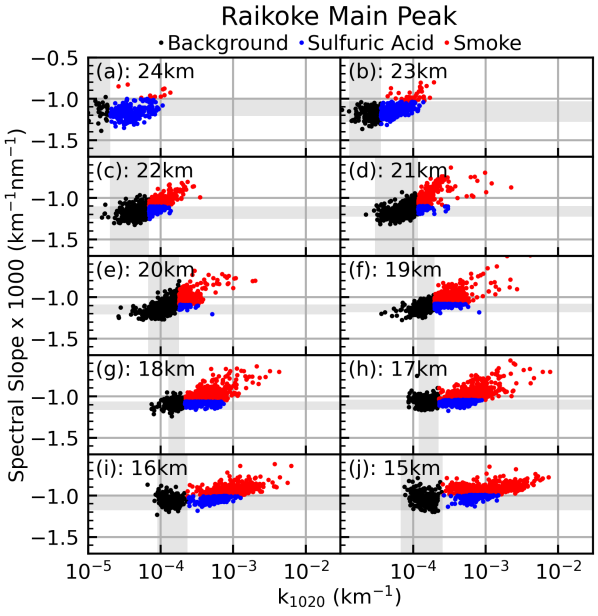

Figure 15. Same as Fig. 7, but for the Raikoke eruption.

continued to circle the globe before it reached a maximum altitude between 23 and 25 km between 10 and 25°N (Chouza et al., 2020). Extinction spectra collected by SAGE between 10°N and 30°N (within 7 months of the eruption) were evaluated to determine the composition of this secondary plume. The results of the altitude-based classification are presented in Fig. 16 as well as the statistics in Table 3.

It is important to recall that the atmosphere had a mixture of aerosol compositions within the Raikoke time period and that a relatively small contribution of smoke can significantly influence the spectral slope as well as k and the degree of this influence is dependent on refractive index. Therefore, the interpretation of Fig. 16 must be done with caution and we have tried, prior to this point, to lay the foundation for this interpretation. In §7.2 we explained how spectra classified as sulfuric acid may have a smoke influence. This was done with a mixed event, such as the Raikoke time period, in mind. Applying this reasoning to the secondary peak allows us to provide a reasonable interpretation of Fig. 16, and we ask the reader to understand that we are not suggesting the data in this case be interpreted as *either* sulfuric acid aerosol *or* smoke; rather there are contributions from both throughout the profiles.

We observed distinctly different patterns between the two case-study event types (i.e., decreasing or near-constant slope with increasing extinction for volcanic events (Figs. 5, 6) and flattening of slope with increasing extinction for wildfire events (Figs. 9, 10)). Both of these general patterns were observed in profiles used in creating Fig. 16, sometimes at the same altitude. For example, the data at 18 and 19 km showed both patterns, which led to a bifurcation in slope at higher extinction coefficients. We interpret this as a mixture of smoke and sulfuric acid aerosol at these altitudes, though not necessarily at the same longitude (i.e., the smoke and sulfuric acid were not necessarily part of the same airmass). That said, what stood out in Fig. 16 was

https://doi.org/10.5194/amt-2021-333
Preprint. Discussion started: 20 October 2021

Atmospheric Measurement Techniques Discussions

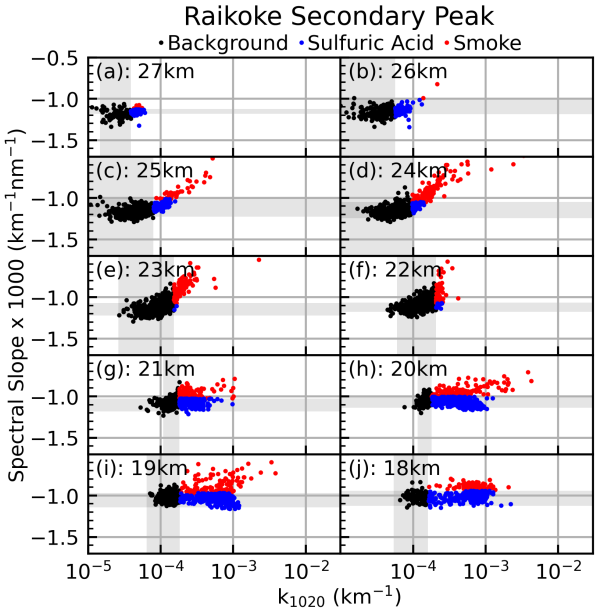

Figure 16. Same as Fig. 5, but for the elevated layer that broke off the main Raikoke plume and continued to ascend as it moved southward.

the dominance of sulfuric acid aerosol at the lowermost altitudes (≤21 km) and the stark transition to a predominantly smoke classification at higher altitudes (>98% at 23 km) where the secondary plume was observed. This transition was most notable between 21 and 25 km where the slope rapidly changed (Fig. 16, panels c-g). While smoke was identified throughout the profile, this partitioning is representative of the behavior expected from single-source events: the absorbing species (smoke) rose to higher altitudes while the non-absorbing species (sulfuric acid) was carried along the same altitude. Further, the presence of smoke throughout the profile demonstrates that the smokey air mass did not traverse through the atmosphere in an isolated manner. Rather, this air mass interacted with the surrounding atmosphere by shedding smoke and likely acquiring sulfuric acid aerosol as it ascended.

Unfortunately comparison with CALIOP was not possible for the secondary plume. Due to the sparseness of SAGE coverage in the tropics an observation that was collocated with CALIOP was not found. However, Chouza et al. (2020) demonstrated that elevated layers in this latitude band were observed from Mauna Loa and CALIOP.

8 Conclusions

We presented a method of distinguishing between sulfuric acid aerosol and smoke using the SAGE III/ISS extinction spectra. This methodology was evaluated using 4 case-study events (2 volcanic, 2 pyroCb) and using the CALIOP depolarization ratio and vertical feature mask. The CALIOP data were supportive of the smoke/sulfuric acid aerosol identification. Identification of aerosol source for the wildfire events was more challenging in that a non-negligible fraction of the spectra were identified as

https://doi.org/10.5194/amt-2021-333
Preprint. Discussion started: 20 October 2021


Atmospheric Measurement Techniques Discussions

sulfuric acid aerosol. However, for the pyroCb events, the spectra with the largest k_{1020} and/or smallest slopes were uniformly identified as smoke.

While we cannot provide a clear definition of magnitude of event required for this method to be applicable, we can state two general cases where it is more likely to fail and the information provided within the introduction should allow the reader to put these events in their proper perspective. First, small wildfire events may not inject enough smoke into the stratosphere to sufficiently change the slope. Similarly, even for large events, if the SAGE sample volume only contains optically thin smoke layers, this too would lead to a sulfuric acid classification. In these cases, we note that classifying these layers as sulfuric acid is not necessarily wrong since the majority of these particles may be composed of background sulfuric acid; this just fails to identify the presence of smoke (i.e., a "false negative" conclusion). Second, during large-scale volcanic eruptions (e.g., Pinatubo with VEI 6), there is a chance for a "false positive" in classifying the resultant sulfuric acid (possibly ash) particles as smoke. Under this scenario, massive amounts of ash and SO_2 is injected into the stratosphere, resulting in formation of large sulfuric acid aerosol particles (e.g., > 500 nm). This would result in a spectrally flat extinction spectrum, which effectively mimics the behavior of smoke in the slope analysis. Usage of this method in either of these conditions is questionable. However, this method is applicable to all events within the SAGE III/ISS record to date.

Interpreting spectra collected during mixed events, such as the combination of the Raikoke eruption and NH pyroCb activity in 2019, presents another challenging case. Ideally, we would understand the composition of these particles, which would provide better understanding for how they interact with light, and we may be able to better model the system. Indeed, in situ sampling of stratospheric smoke would prove valuable for improving this method as well as improving climate and chemistry models. However, with these limitations in mind, we presented a framework for interpreting data from mixed events that allows the reader to understand not only the assumptions herein, but the conditions under which conclusions are either reasonable or tenuous.

Finally, we demonstrated that the secondary plume that broke off from the main Raikoke plume and moved southward was composed primarily of smoke while the aerosol at lower altitudes was predominantly sulfuric acid with a smaller contribution from smoke. This is supportive of the initial hypothesis that the secondary plume was composed of smoke and suggests that the smoke and sulfuric acid particles separated as they moved southward: smoke continued to loft to higher altitudes while sulfuric acid stayed at lower altitudes. While these two aerosol types separated, they did not do so perfectly. Indeed, we identified traces of smoke in the lower altitudes and sulfuric acid aerosol at the higher altitudes. The general pattern we observed is that these species separated in a manner that is consistent with the expected behavior based on their refractive index values.

Data availability. The SAGE and CALIOP data used within this study are available on NASA's Atmospheric Science Data Center (https://eosweb.larc.nasa.gov/).

https://doi.org/10.5194/amt-2021-333
Preprint. Discussion started: 20 October 2021

Atmospheric Measurement Techniques Discussions

Author contributions. TNK and LT developed the methodology, while TNK carried out the analysis, wrote the analysis code and the manuscript. RD, MK, DF, JT, and JK participated in scientific discussions and provided guidance throughout the study. JT and JK provided guidance on the use and interpretation of the CALIOP data. All authors reviewed the manuscript during the preparation process

Competing interests. The authors declare that they have no competing interests.

Acknowledgements. SAGE III/ISS is a NASA Langley managed mission funded by the NASA Science Mission Directorate within the Earth Systematic Mission Program. Enabling partners are the NASA Human Exploration and Operations Mission Directorate, International Space Station Program and the European Space Agency. SSAI personnel are supported through the STARSS III contract NNL16AA05C.

https://doi.org/10.5194/amt-2021-333
Preprint. Discussion started: 20 October 2021

Atmospheric Measurement Techniques Discussions

References

Bachmeier, Scott: PyroCb in Russia, http://pyrocb.ssec.wisc.edu/archives/2321, accessed: 2021-02-23, 2019.

Bergstrom, R. W., Russell, P. B., and Hignett, P.: Wavelength Dependence of the Absorption of Black Carbon Particles: Predictions and Results from the TARFOX Experiment and Implications for the Aerosol Single Scattering Albedo, Journal of the Atmospheric Sciences, 59, 567–577, https://doi.org/10.1175/1520-0469(2002)059<0567:WDOTAO>2.0.CO;2, 2002.

Bluth, G. J. S., Doiron, S. D., Schnetzler, C. C., Krueger, A. J., and Walter, L. S.: Global tracking of the SO2 clouds from the June, 1991 Mount Pinatubo eruptions, Geophysical Research Letters, 19, 151–154, https://doi.org/10.1029/91GL02792, 1992.

Boers, R., de Laat, A. T., Stein Zweers, D. C., and Dirksen, R. J.: Lifting potential of solar-heated aerosol layers, Geophysical Research Letters, 37, L24 802, https://doi.org/10.1029/2010GL045171, 2010.

Chagnon, C. and Junge, C.: The Vertical Distribution of Sub-Micron Particles in the Stratosphere, Journal of Meteorology, 18, 746–752, https://doi.org/10.1175/1520-0469(1961)018<0746:TVDOSM>2.0.CO;2, 1961.

Chouza, F., Leblanc, T., Barnes, J., Brewer, M., Wang, P., and Koon, D.: Long-term (1999–2019) variability of stratospheric aerosol over Mauna Loa, Hawaii, as seen by two co-located lidars and satellite measurements, Atmospheric Chemistry and Physics, 20, 6821–6839, https://doi.org/10.5194/acp-20-6821-2020, 2020.

Christian, K., Yorks, J., and Das, S.: Differences in the Evolution of Pyrocumulonimbus and Volcanic Stratospheric Plumes as Observed by CATS and CALIOP Space-Based Lidars, Atmosphere, 11, https://doi.org/10.3390/atmos11101035, 2020.

Cisewski, M., Zawodny, J., Gasbarre, J., Eckman, R., Topiwala, N., Rodriguez-Alvarez, O., Cheek, D., and Hall, S.: The Stratospheric Aerosol and Gas Experiment (SAGE III) on the International Space Station (ISS) Mission, in: Sensors, Systems, and Next-Generation Satellites XVIII, edited by Meynart, R and Neeck, SP and Shimoda, H, vol. 9241 of *Proceedings of SPIE*, p. 924107, SPIE, https://doi.org/10.1117/12.2073131, Conference on Sensors, Systems, and Next-Generation Satellites XVIII, Amsterdam, Netherlands, Sep 22-25, 2014, 2014.

D'Arrigo, R., Seager, R., Smerdon, J. E., LeGrande, A. N., and Cook, E. R.: The anomalous winter of 1783–1784: Was the Laki eruption or an analog of the 2009–2010 winter to blame?, Geophysical Research Letters, 38, L05 706, https://doi.org/10.1029/2011GL046696, 2011.

de Laat, A. T. J., Stein Zweers, D. C., Boers, R., and Tuinder, O. N. E.: A solar escalator: Observational evidence of the self-lifting of smoke and aerosols by absorption of solar radiation in the February 2009 Australian Black Saturday plume, Journal of Geophysical Research: Atmospheres, 117, D04 204, https://doi.org/10.1029/2011JD017016, 2012.

de Leeuw, J., Schmidt, A., Witham, C. S., Theys, N., Taylor, I. A., Grainger, R. G., Pope, R. J., Haywood, J., Osborne, M., and Kristiansen, N. I.: The 2019 Raikoke volcanic eruption: Part 1 Dispersion model simulations and satellite retrievals of volcanic sulfur dioxide, Atmospheric Chemistry and Physics Discussions, 2020, 1–38, https://doi.org/10.5194/acp-2020-889, 2020.

de Leeuw, J., Schmidt, A., Witham, C. S., Theys, N., Taylor, I. A., Grainger, R. G., Pope, R. J., Haywood, J., Osborne, M., and Kristiansen, N. I.: The 2019 Raikoke volcanic eruption – Part 1: Dispersion model simulations and satellite retrievals of volcanic sulfur dioxide, Atmospheric Chemistry and Physics, 21, 10 851–10 879, https://doi.org/10.5194/acp-21-10851-2021, 2021.

Deshler, T., Hervig, M., Hofmann, D., Rosen, J., and Liley, J.: Thirty years of in situ stratospheric aerosol size distribution measurements from Laramie, Wyoming (41°N), using balloon-borne instruments, Journal of Geophysical Research-Atmospheres, 108, 4167, https://doi.org/10.1029/2002JD002514, 2003.

Fromm, M., Tupper, A., Rosenfeld, D., Servranckx, R., and McRae, R.: Violent pyro-convective storm devastates Australia's capital and pollutes the stratosphere, Geophysical Research Letters, 33, L05 815, https://doi.org/10.1029/2005GL025161, 2006.

https://doi.org/10.5194/amt-2021-333
Preprint. Discussion started: 20 October 2021

Fromm, M., Lindsey, D. T., Servranckx, R., Yue, G., Trickl, T., Sica, R., Doucet, P., and Godin-Beekmann, S.: The Untold Story of Pyrocumulonimbus, Bulletin of the American Meteorological Society, 91, 1193–1210, https://doi.org/10.1175/2010BAMS3004.1, 2010.

Getzewich, B. J., Vaughan, M. A., Hunt, W. H., Avery, M. A., Powell, K. A., Tackett, J. L., Winker, D. M., Kar, J., Lee, K.-P., and Toth, T. D.: CALIPSO lidar calibration at 532 nm: version 4 daytime algorithm, Atmospheric Measurement Techniques, 11, 6309–6326, https://doi.org/10.5194/amt-11-6309-2018, 2018.

Hedelt, P., Efremenko, D. S., Loyola, D. G., Spurr, R., and Clarisse, L.: Sulfur dioxide layer height retrieval from Sentinel-5 Precursor/TROPOMI using FP_ILM, Atmospheric Measurement Techniques, 12, 5503–5517, https://doi.org/10.5194/amt-12-5503-2019, 2019.

Johnston, F. H., Borchers-Arriagada, N., Morgan, G. G., Jalaludin, B., Palmer, A. J., Williamson, G. J., and Bowman, D. M. J. S.: Unprecedented health costs of smoke-related PM2.5 from the 2019-20 Australian megafires, Nature Sustainability, 4, 42–47, https://doi.org/10.1038/s41893-020-00610-5, 2020.

Kablick III, G. P., Allen, D. R., Fromm, M. D., and Nedoluha, G. E.: Australian PyroCb Smoke Generates Synoptic-Scale Stratospheric Anticyclones, Geophysical Research Letters, 47, e2020GL088 101, https://doi.org/10.1029/2020GL088101, 2020.

Kar, J., Vaughan, M. A., Kam-Pui, L., Tackett, J. L., Avery, M. A., Garnier, A., Getzewich, B. J., Hunt, W. H., Josset, D., Liu, Z., et al.: CALIPSO lidar calibration at 532 nm: version 4 nighttime algorithm, Atmospheric Measurement Techniques, 11, 1459–1479, https://doi.org/10.5194/amt-11-1459-2018, 2018.

Kar, J., Lee, K.-P., Vaughan, M. A., Tackett, J. L., Trepte, C. R., Winker, D. M., Lucker, P. L., and Getzewich, B. J.: CALIPSO level 3 stratospheric aerosol profile product: version 1.00 algorithm description and initial assessment, Atmospheric Measurement Techniques, 12, 6173–6191, https://doi.org/10.5194/amt-12-6173-2019, 2019.

Kim, M.-H., Omar, A. H., Tackett, J. L., Vaughan, M. A., Winker, D. M., Trepte, C. R., Hu, Y., Liu, Z., Poole, L. R., Pitts, M. C., Kar, J., and Magill, B. E.: The CALIPSO version 4 automated aerosol classification and lidar ratio selection algorithm, Atmospheric Measurement Techniques, 11, 6107–6135, https://doi.org/10.5194/amt-11-6107-2018, 2018.

Kloss, C., Berthet, G., Sellitto, P., Ploeger, F., Taha, G., Tidiga, M., Eremenko, M., Bossolasco, A., Jégou, F., Renard, J.-B., and Legras, B.: Stratospheric aerosol layer perturbation caused by the 2019 Raikoke and Ulawun eruptions and their radiative forcing, Atmospheric Chemistry and Physics, 21, 535–560, https://doi.org/10.5194/acp-21-535-2021, 2021.

Knepp, T. N., Thomason, L., Roell, M., Damadeo, R., Leavor, K., Leblanc, T., Chouza, F., Khaykin, S., Godin-Beekmann, S., and Flittner, D.: Evaluation of a Method for Converting SAGE Extinction Coefficients to Backscatter Coefficient for Intercomparison with LIDAR Observations, Atmospheric Measurement Techniques Discussions, 2020, 1–24, https://doi.org/10.5194/amt-2020-60, 2020.

Kozlov, V. S., Yausheva, E. P., Terpugova, S. A., Panchenko, M. V., Chernov, D. G., and Shmargunov, V. P.: Optical–microphysical properties of smoke haze from Siberian forest fires in summer 2012, International Journal of Remote Sensing, 35, 5722–5741, https://doi.org/10.1080/01431161.2014.945010, 2014.

Kremser, S., Thomason, L. W., von Hobe, M., Hermann, M., Deshler, T., Timmreck, C., Toohey, M., Stenke, A., Schwarz, J. P., Weigel, R., Fueglistaler, S., Prata, F. J., Vernier, J.-P., Schlager, H., Barnes, J. E., Antuna-Marrero, J.-C., Fairlie, D., Palm, M., Mahieu, E., Notholt, J., Rex, M., Bingen, C., Vanhellemont, F., Bourassa, A., Plane, J. M. C., Klocke, D., Carn, S. A., Clarisse, L., Trickl, T., Neely, R., James, A. D., Rieger, L., Wilson, J. C., and Meland, B.: Stratospheric aerosol-Observations, processes, and impact on climate, Reviews of Geophysics, 54, 278–335, https://doi.org/10.1002/2015RG000511, 2016.

Leys, C., Ley, C., Klein, O., Bernard, P., and Licata, L.: Detecting outliers: Do not use standard deviation around the mean, use absolute deviation around the median, Journal of Experimental Social Psychology, 49, 764–766, https://doi.org/10.1016/j.jesp.2013.03.013, 2013.

https://doi.org/10.5194/amt-2021-333
Preprint. Discussion started: 20 October 2021

McCormick, M., Thomason, L., and Trepte, C.: Atmospheric Effects of the Mt-Pinatubo Eruption, Nature, 373, 399–404, https://doi.org/10.1038/373399a0, 1995.

Müller, D., Mattis, I., Wandinger, U., Ansmann, A., Althausen, D., and Stohl, A.: Raman lidar observations of aged Siberian and Canadian forest fire smoke in the free troposphere over Germany in 2003: Microphysical particle characterization, Journal of Geophysical Research: Atmospheres, 110, D17 201, https://doi.org/10.1029/2004JD005756, 2005.

Murphy, D., Thomson, D., and Mahoney, T.: In situ measurements of organics, meteoritic material, mercury, and other elements in aerosols at 5 to 19 kilometers, Science, 282, 1664–1669, https://doi.org/10.1126/science.282.5394.1664, 1998.

Muser, L. O., Hoshyaripour, G. A., Bruckert, J., Horvath, A., Malinina, E., Peglow, S., Prata, F. J., Rozanov, A., von Savigny, C., Vogel, H., and Vogel, B.: Particle Aging and Aerosol–Radiation Interaction Affect Volcanic Plume Dispersion: Evidence from Raikoke Eruption 2019, Atmospheric Chemistry and Physics Discussions, 2020, 1–27, https://doi.org/10.5194/acp-2020-370, 2020.

Newhall, C. G. and Self, S.: The volcanic explosivity index (VEI) an estimate of explosive magnitude for historical volcanism, Journal of Geophysical Research: Oceans, 87, 1231–1238, https://doi.org/10.1029/JC087iC02p01231, 1982.

Palmer, K. and Williams, D.: Optical-Constants of Sulfuric-Acid - Application to Clouds of Venus, Applied Optics, 14, 208–219, https://doi.org/10.1364/AO.14.000208, 1975.

Park, Y. H., Sokolik, I. N., and Hall, S. R.: The impact of smoke on the ultraviolet and visible radiative forcing under different fire regimes, Air, Soil and Water Research, 11, 1–10, https://doi.org/10.1177/1178622118774803, 2018.

Peterson, D., R. Campbell, J., Hyer, E., D. Fromm, M., P. Kablick, G., H. Cossuth, J., and Deland, M.: Wildfire-driven thunderstorms cause a volcano-like stratospheric injection of smoke, npj Climate and Atmospheric Science, 1, , https://doi.org/10.1038/s41612-018-0039-3, 2018.

Pinto, J. P., Turco, R. P., and Toon, O. B.: Self-limiting physical and chemical effects in volcanic eruption clouds, Journal of Geophysical Research: Atmospheres, 94, 11 165–11 174, https://doi.org/10.1029/JD094iD08p11165, 1989.

Pitts, M. and Thomason, L.: The Impact of the Eruptions of Mount-Pinatubo and Cerro Hudson on Antarctic Aerosol Levels During the 1991 Austral Spring, Geophysical Research Letters, 20, 2451–2454, https://doi.org/10.1029/93GL02160, 1993.

Pyle, D. M.: Mass and energy budgets of explosive volcanic eruptions, Geophysical Research Letters, 22, 563–566, https://doi.org/10.1029/95GL00052, 1995.

Rashidov, V., Girina, O., Ozerov, A. Y., and Pavlov, N.: The June 2019. Eruption of Raikoke volcano (the Kurile Islands), Bulletin of Kamchatka Regional Association "Educational-Scientific Center". Earth Sciences, 42, 5–8, 2019.

Santer, B. D., Bonfils, C., Painter, J. F., Zelinka, M. D., Mears, C., Solomon, S., Schmidt, G. A., Fyfe, J. C., Cole, J. N., Nazarenko, L., et al.: Volcanic contribution to decadal changes in tropospheric temperature, Nature Geoscience, 7, 185–189, https://doi.org/10.1038/NGEO2098, 2014.

Schurer, A. P., Hegerl, G. C., Luterbacher, J., Brönnimann, S., Cowan, T., Tett, S. F. B., Zanchettin, D., and Timmreck, C.: Disentangling the causes of the 1816 European year without a summer, Environmental Research Letters, 14, 094 019, https://doi.org/10.1088/1748-9326/ab3a10, 2019.

Stothers, R. B.: The Great Tambora Eruption in 1815 and Its Aftermath, Science, 224, 1191–1198, https://doi.org/10.1126/science.224.4654.1191, 1984.

Sumlin, B. J., Heinson, Y. W., Shetty, N., Pandey, A., Pattison, R. S., Baker, S., Hao, W. M., and Chakrabarty, R. K.: UV–Vis–IR spectral complex refractive indices and optical properties of brown carbon aerosol from biomass burning, Journal of Quantitative Spectroscopy and Radiative Transfer, 206, 392–398, https://doi.org/https://doi.org/10.1016/j.jqsrt.2017.12.009, 2018.

https://doi.org/10.5194/amt-2021-333
Preprint. Discussion started: 20 October 2021

Tanakadate, H.: The volcanic activity of Japan during 1914-1924, Bulletin Volcanologique, 1, 3–19, https://doi.org/10.1007/BF02719558, 1925.

Thomason, L.: Observations of a New SAGE-II Aerosol Extinction Mode Following the Eruption of Mt-Pinatubo, Geophysical Research Letters, 19, 2179–2182, https://doi.org/10.1029/92GL02185, 1992.

Thomason, L. W., Kovilakam, M., Schmidt, A., von Savigny, C., Knepp, T., and Rieger, L.: Evidence for the predictability of changes in the stratospheric aerosol size following volcanic eruptions of diverse magnitudes using space-based instruments, Atmospheric Chemistry and Physics, 21, 1143–1158, https://doi.org/10.5194/acp-21-1143-2021, 2021.

Thomason, L. W., Burton, S. P., Luo, B. P., and Peter, T.: SAGE II measurements of stratospheric aerosol properties at non-volcanic levels, Atmospheric Chemistry and Physics, 8, 983–995, https://doi.org/10.5194/acp-8-983-2008, 2008.

Thordarson, T. and Self, S.: The Laki (Skaftár Fires) and Grímsvötn eruptions in 1783–1785, Bulletin of Volcanology, 55, 233–263, 1993.

Thordarson, T. and Self, S.: Atmospheric and environmental effects of the 1783–1784 Laki eruption: A review and reassessment, Journal of Geophysical Research: Atmospheres, 108, AAC 7–1–AAC 7–29, https://doi.org/10.1029/2001JD002042, 2003.

Turco, R. P., Toon, O. B., Ackerman, T. P., Pollack, J. B., and Sagan, C.: Nuclear winter: Global consequences of multple nuclear explosions, Science, 222, 1283–1292, 1983.

Vaughan, G., Wareing, D., and Ricketts, H.: Measurement Report: Lidar measurements of stratospheric aerosol following the 2019 Raikoke and Ulawun volcanic eruptions, Atmospheric Chemistry and Physics, 21, 5597–5604, https://doi.org/10.5194/acp-21-5597-2021, 2021.

Vaughan, M., Pitts, M., Trepte, C., Winker, D., Detweiler, P., Garnier, A., Getzewich, B., Hunt, W., Lambeth, J., Lee, K.-P., Lucker, P., Murray, T., Rodier, S., Tremas, T., Bazureau, A., and Pelon, J.: Cloud –Aerosol LIDAR Infrared Pathfinder Satellite Observations: Data Management System, Data Products Catalog, Release 4.30, Report, National Aeronautics and Space Administration, accessed: 2021-05-27, 2018.

Vernier, J. P., Thomason, L. W., Pommereau, J. P., Bourassa, A., Pelon, J., Garnier, A., Hauchecorne, A., Blanot, L., Trepte, C., Degenstein, D., and Vargas, F.: Major influence of tropical volcanic eruptions on the stratospheric aerosol layer during the last decade, Geophysical Research Letters, 38, L12 807, https://doi.org/10.1029/2011GL047563, 2011.

Wang, H. J. R., Damadeo, R., Flittner, D., Kramarova, N., Taha, G., Davis, S., Thompson, A. M., Strahan, S., Wang, Y., Froidevaux, L., Degenstein, D., Bourassa, A., Steinbrecht, W., Walker, K. A., Querel, R., Leblanc, T., Godin-Beekmann, S., Hurst, D., and Hall, E.: Validation of SAGE III/ISS Solar Occultation Ozone Products With Correlative Satellite and Ground-Based Measurements, Journal of Geophysical Research: Atmospheres, 125, e2020JD032 430, https://doi.org/10.1029/2020JD032430, e2020JD032430 2020JD032430, 2020.

Wilka, C., Shah, K., Stone, K., Solomon, S., Kinnison, D., Mills, M., Schmidt, A., and Neely, III, R. R.: On the Role of Heterogeneous Chemistry in Ozone Depletion and Recovery, Geophysical Research Letters, 45, 7835–7842, https://doi.org/10.1029/2018GL078596, 2018.

Winker, D., Pelon, J., Coakley Jr, J., Ackerman, S., Charlson, R., Colarco, P., Flamant, P., Fu, Q., Hoff, R., Kittaka, C., et al.: The CALIPSO mission: A global 3D view of aerosols and clouds, Bulletin of the American Meteorological Society, 91, 1211–1230, https://doi.org/10.1175/2010BAMS3009.1, 2010.

Witham, C. S. and Oppenheimer, C.: Mortality in England during the 1783–4 Laki Craters eruption, Bulletin of Volcanology, 67, 15–26, 2004.

Womack, C. C., Manfred, K. M., Wagner, N. L., Adler, G., Franchin, A., Lamb, K. D., Middlebrook, A. M., Schwarz, J. P., Brock, C. A., Brown, S. S., and Washenfelder, R. A.: Complex refractive indices in the ultraviolet and visible spectral region for highly absorbing

https://doi.org/10.5194/amt-2021-333
Preprint. Discussion started: 20 October 2021


Atmospheric Measurement Techniques Discussions

630 non-spherical biomass burning aerosol, Atmospheric Chemistry and Physics, 21, 7235–7252, https://doi.org/10.5194/acp-21-7235-2021, 2021.

Yu, P., Toon, O., Bardeen, C., Zhu, Y., Rosenlof, K., Portmann, R., Thornberry, T., Gao, R.-S., Davis, S., Wolf, E., de Gouw, J., Peterson, D., Fromm, M., and Robock, A.: Black carbon lofts wildfire smoke high into the stratosphere to form a persistent plume, Science, 365, 587–590, https://doi.org/10.1126/science.aax1748, 2019.